Eccentric Poisson-Boltzmann cell model

H. H. von Grünberg
Fakultät für Physik, Universität Konstanz, 78457 Konstanz, Germany

L. Belloni
CEA/SACLAY, Service de Chimie Moléculaire, 91191 Gif sur Yvette, Cedex, France

(Received 11 April 2000)

We solve the nonlinear Poisson-Boltzmann equation around a charged colloidal sphere in an electrolyte that is confined in a cell. The colloid has an eccentric position inside the confining sphere. This models the situation in a highly concentrated charge-stabilized colloidal suspension, where a single colloid simultaneously interacts with the whole cage of neighboring colloids. We calculate the ion density profiles, the free energy, and the osmotic pressure as a function of the shifting position. We express the total force acting on the particle as a sum of pair contributions and compare the resulting pair interaction potential law with the standard Derjaguin-Landau-Verwey-Overbeck expression.

PACS number(s): 61.20.Qg, 82.45.+z

I. INTRODUCTION

In charged colloidal or polyelectrolyte solutions, there are three different types of particles: polyions, microions, and the molecules of the solvent. Due to the enormous size and charge asymmetry between these three species, not all of them are equally important for the interpretation of the experimental data. In light scattering experiments, for instance, it is only the time-averaged positions of the mesoscopic polyions that is of significance to the measured structure factors. In many cases it is therefore sufficient to give an effective one-component description of the mixture, that is, to treat the polyion plus its microionic atmosphere as one dressed particle that moves in a dielectric medium [1]. In this approach, the central question is to know about the solvent and microion-averaged or effective potential between these dressed particles [2–4].

In highly diluted suspensions with added salt, the colloids interact essentially by pairs. The effective pair potential which results from the overlap of two ionic double layers can be calculated in a good approximation (for monovalent ions) from the nonlinear Poisson-Boltzmann (PB) equation [5,6]. At large separation, the weak overlap or linear superposition approximation applies and the potential takes the usual screened-Coulombic Yukawa Derjaguin-Landau-Verwey-Overbeck (DLVO) form [7]. In this expression, the bare charge is replaced by the effective value which accounts for the electrostatic condensation of counterions near the colloids and which can be deduced from the PB solution around one isolated particle [8,9,1,10]. The DLVO potential has been extensively used to describe the phase behavior [11], structure [12,13], dynamics [14], and electrokinetic properties [15] of charged colloidal suspensions, even outside the dilute regime. However, for concentrated and/or salt-free solutions, this asymptotic pair potential becomes, in principle, incorrect: first, the linear superposition approximation breaks down due to the strong overlap of the double layers and of the condensation shells at short separations [5]; more importantly, many simultaneously overlapping layers lead to effective forces that are essentially many body in nature; i.e., the force between two particles will depend also on the positions of all other polyions. Thus, the problem becomes rather involved, not only for the technical problems posed by the demanding nonlinear PB equation, but also because, in principle, the total interaction can no longer be split into pairwise contributions.

In the present article we concentrate on this high concentration limit. In a complete PB theory one would have to solve the nonlinear PB equation in the interstitial regions between all colloidal spheres for each possible colloidal configuration. This requires a formidable numerical treatment [16,17]. We rather investigate a simpler geometry made of a single colloid interacting with the entire cage of surrounding polyions. To model this situation, we consider a charged colloid located at eccentric positions inside a hollow charged sphere. The inhomogeneous electrolyte fills the volume between the two nonconcentric surfaces. The confining sphere represents the fixed cage of next neighbors of a colloid in the suspension. Next to this outer sphere another double layer of microions will be formed, which may be regarded as the superposed double layers of all neighbors defining the cage. The overlap of this concave layer with the convex layer around the center colloid leads to a repulsive force which drives the colloid back toward the center of the cell. We calculate this force and related quantities by solving the PB equation for the electrostatic potential and ionic profiles in the eccentric cell geometry. A similar problem can be found in an old study by Ohtsuki et al. [18] where the electrostatic potential around a particle in an ordered latex under a deformation has been numerically calculated.

The total force acting on the central colloid is not a pair force but the accumulated force of all neighbors onto the center colloid. However, we suggest a way how this force can again be decomposed into pair forces. The resulting pair potentials can be compared to the pair potentials derived in the conventional way from the overlap of two spherical double layers with positive curvature. We thus end up with an effective ion-averaged potential for two colloids interacting in the immediate neighborhood of other colloids, the influence of whose double layers on the interaction of the two

colloids we explicitly take into account. This approach, of course, makes sense only in highly concentrated suspensions. From these considerations, it should be clear that we have to expect a qualitatively different behavior of the effective interaction.

After setting the stage for our considerations in Sec. II, we introduce in Sec. III our model, which we call the ''eccentric cell model,'' and present in Sec. IV the calculated density profiles. From these, we determine in Sec. V the forces by integrating the stress tensor, and decompose these into pair forces in Sec. VI. Before the conclusion, we shortly discuss in Sec. VII the osmotic pressure of the suspension in the eccentric cell model.

II. POISSON-BOLTZMANN THEORY

We consider a colloidal suspension made of N_p spherical charged colloids. Their density is $n_p=N_p/V=1/V_{WS}$, where V_{WS} is the volume per colloid or, in the crystalline phase, the volume of the Wigner-Seitz (WS) cell. Each colloidal particle bears a charge of $+Ze$. Assuming, for simplicity, that the charge of a counterion is $-e$, each colloid thus contributes Z counterions to the solution, giving in total $N_c=ZN_p$ counterions and hence a counterion density of $n_c=N_c/V$. Additionally, we allow for a binary symmetrical $1/-1$ salt of concentration $n_s=S/V_{WS}$ to be present where S is the number of positive/negative salt ions in the Wigner-Seitz cell volume. As usual, the solvent (water) is assumed to be a continuum of dielectric constant ϵ (primitive model), while the microions are considered to be pointlike particles.

Mapping the initial multicomponent system onto an effective one-component system made of dressed colloids, we may write the total free energy for a given position $\{\vec{R}_i\}$ of all N_p colloidal particles in the form $\mathcal{F}(\{\vec{R}_i\})$. The average over the degrees of freedom of the microions, implicitly taken into account in $\mathcal{F}$, is performed here within the mean-field PB approximation. The microion-microion correlations are neglected and the inhomogeneous ionic density profiles $\rho_+(\vec{r})$ and $\rho_-(\vec{r})$ in the external field of the macroions (fixed at $\{\vec{R}_i\}$) are related to the normalized averaged electrostatic potential Φ through the mean-field Boltzmann relations $\rho_\mp(\vec{r})\propto\exp[\pm\Phi(\vec{r})]$. The PB equation reads

$$\nabla^2\Phi(\vec{r})=4\pi\lambda_B[\rho_-(\vec{r})-\rho_+(\vec{r})]$$
$$=4\pi\lambda_B\left[(n_s+n_c)\frac{e^{\Phi(\vec{r})}}{\langle e^{\Phi(\vec{r})}\rangle}-n_s\frac{e^{-\Phi(\vec{r})}}{\langle e^{-\Phi(\vec{r})}\rangle}\right], \quad (1)$$

where $\Phi=e\beta\Psi$ is the electrostatic potential, $\lambda_B=e^2\beta/\epsilon$ the Bjerrum length, and $\beta=1/k_BT$ the inverse temperature. The volume averages (brackets) guarantee the total ionic conservation (fixed salinity inside the solution). The PB total free energy of the solution which depends on the colloidal configuration reads [7]

$$\mathcal{F}(\{\vec{R}_i\})=\int d\vec{r}'\left[\frac{\epsilon}{8\pi}E^2(\vec{r}')\right.$$
$$\left.+\sum_{\alpha=\pm}\rho_\alpha(\vec{r}')k_BT[\ln\{\Lambda^3\rho_\alpha(\vec{r}')\}-1]\right], \quad (2)$$

with $\vec{E}$ being the total electric field and Λ the thermal de Broglie wavelength. The first term is the Coulomb energy of the charged colloids and their microions, while the second term takes account of the ideal-gas entropy of mixture of the discrete microions. The Boltzmann profiles are those which minimize the free energy of Eq. (2) seen as a functional of the variational densities $\rho_\pm(r)$ (at fixed total ionic content).

The force $\vec{F}_j$ acting on colloid j derives from the free energy:

$$\vec{F}_j=-\vec{\nabla}_j\mathcal{F}(\{\vec{R}_i\}). \quad (3)$$

Both the free energy $\mathcal{F}$ and the forces $\vec{F}_j$ are complex N_p-body quantities which, in general, cannot be decomposed as sums of pair contributions. Meanwhile, for conceptual and practical reasons, it is interesting to define the effective pair potential v^{eff} which, when being summed over all interparticle distances $R_{ij}=|\vec{R}_i-\vec{R}_j|$, gives the best approximation possible to the energy of Eq. (2),

$$\mathcal{F}(\{\vec{R}_i\})\approx\mathcal{F}_0+\sum_{i<j}v^{eff}(R_{ij}). \quad (4)$$

The term $\mathcal{F}_0$, independent of the colloidal positions, is irrelevant for the interactions and forces [20,21].

In the weak overlap approximation valid at large interparticle distances, the microionic density distributions turn out to be given by sums over independent distributions around isolated colloids and the pairwise decomposition, Eq. (4), applies. Placing this sum into the free energy expression, Eq. (2), gives for the effective pair potential the DLVO form

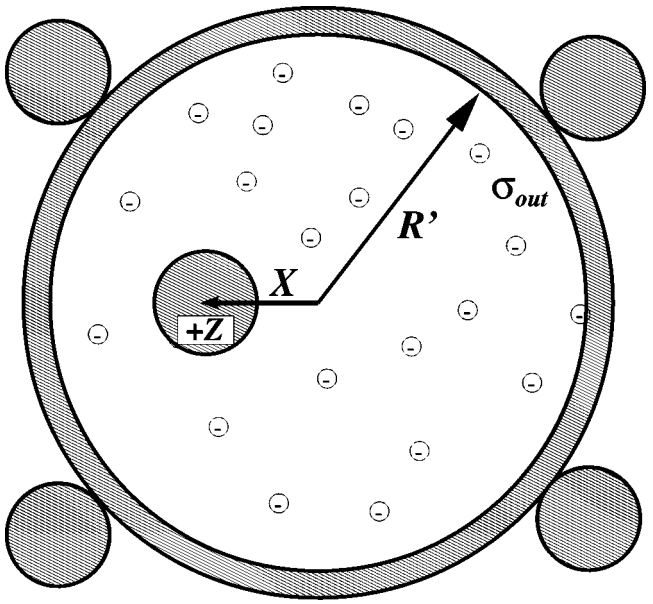

FIG. 1. The eccentric cell model: a positively charged colloid is shifted a distance X from the center of a spherical cage. The outer surface bears a positive surface charge density σ_{out}. The cavity radius $R'=2R-a$ where a is the radius of the colloid and R is defined through the volume per colloid, $V_{WS}=4\pi R^3/3$. The shell of next neighbors is at $2R$.

$$\beta v^{eff}(R)=\left(Z_{eff}\frac{e^{\kappa a}}{1+\kappa a}\right)^2\lambda_B\frac{e^{-\kappa R}}{R},\quad R>2a, \qquad (5)$$

with a being the radius of the colloidal sphere and $\kappa=[4\pi\lambda_B(n_c+2n_s)]^{1/2}$ the inverse screening length.

The effective charge Z_{eff} in Eq. (5) is equal to the bare charge Z within the linear PB (Debye-Hückel) theory and is much lower than Z in the nonlinear theory due to the counterionic condensation. At small interparticle distances observed in concentrated solutions, the DLVO potential is, in principle, less valid and the pairwise decomposition, Eq. (4), though practical, is more approximative.

III. ECCENTRIC CELL MODEL

We see from Eq. (2) that, in principle, one has to solve the multicentered PB equation for every possible colloidal configuration. Though not impossible [16,17], this can only be achieved with a large scale computer simulation. Contrary to that, the basic idea of the PB cell model is convincingly easy. There, only one specific colloidal configuration is considered, namely, the fcc configuration of the crystalline phase, so that due to the translational symmetry the nonlinear PB equation for the microionic density distribution needs to be calculated in one WS cell only.

Assuming the WS cell to be of spherical shape (radius R defined via $4\pi R^3/3=V_{WS}$), the problem then reduces to solving the radial one-dimensional PB equation and one is left with the following von Neumann boundary value problem (BVP):

$$\frac{1}{r^2}\partial_r r^2\partial_r\Phi(r)=4\pi\lambda_B\left[(n_s+n_c)\frac{e^{\Phi(\vec{r})}}{\langle e^{\Phi(\vec{r})}\rangle}-n_s\frac{e^{-\Phi(\vec{r})}}{\langle e^{-\Phi(\vec{r})}\rangle}\right],$$

$$\partial_r\Phi(r)|_{r=R}=0, \qquad (6)$$

$$\partial_r\Phi(r)|_{r=a}=-\frac{Z\lambda_B}{a^2},$$

where the first boundary value reflects the fact that the WS sphere as a whole is electrically neutral (all Z counterions are inside R) and the second is just the constant-charge boundary condition at the colloid surface commonly used for colloidal particles. This classical cell approach is powerful to derive ionic profiles, osmotic pressures, and effective charges in concentrated solutions. On the other hand, due to its spherical symmetry, it is unsuited for deriving directly colloidal forces and colloid-colloid interactions.

The idea of our eccentric cell model (see Fig. 1) may be seen as an extension of this centric PB cell model. We also start from the assumption that all macroions are initially located at fcc lattice sites. However, in contrast to the conventional cell model, we allow one colloid to be shifted a distance X from its center position. Calculating for each X the PB profiles, one can then determine $\mathcal{F}$, Eq. (2), and, from its derivative, Eq. (3), directly the force acting on the colloid.

Of crucial importance is a physically motivated choice of the boundary condition: The boundary condition at R in Eq. (6) cannot be copied in the eccentric geometry. Since the central colloid is shifted a distance X while the 12 neighbors

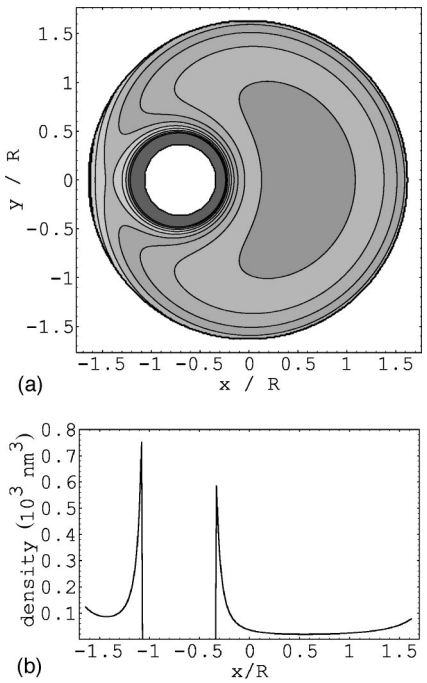

FIG. 2. (a) Typical ion density distribution as calculated from the mean-field Poisson-Boltzmann equation for a colloidal macroion in the eccentric geometry ($Z=600$, $a=500$ Å, volume fraction $\phi=0.05$, $X=0.69R$, $S=0$, $\lambda_B=7.2$ Å). (b) A cut at $y=0$ along the x axis for the distribution of (a). Units are in R throughout.

are kept fixed, one expects that the normal electric field is zero at $r>R$ in the sense of the shift and at $r<R$ in the opposite sense (r is measured from the center of the cell). We therefore enlarge the spherical cell to a radius $R'=2R-a$ and consider the *whole cage* consisting of all 12 neighbors (at $2R$) around the central colloid, rather than the central WS cell alone, because the position of the whole cage will certainly not depend on X. The 12 neighbors are replaced by a spherical charged surface at R' that is concentric with the original WS sphere (see Fig. 1). This leads to the picture presented in the introduction: a single colloid trapped in the spherical cage of its nearest neighbors. The procedure in practice is the following: in a first step, the centered PB solution $\Phi(r)$ of the BVP in Eq. (6), unperturbed in the central WS cell $r<R$, is extended until $r=R'$ by integrating the same PB equation from $r=R$ to $r=R'$. The nonzero electric field at $r=R'$ gives, with the Gauss theorem, the surface charge density σ_{out} of the outer cell surface (due to the finite spherical curvature of the configuration, σ_{out} differs from the colloidal surface charge density at $r=a$). Then, in the eccentric geometry, this charge density and the corresponding normal electric field at $r=R'$ are kept fixed as the central colloid is shifted away from its initial position. This choice for the boundary condition matches closely what happens in a real cage while keeping the spherical cell geometry.

Since there is still a rotational symmetry about the line joining the center of the WS sphere and the center of the colloidal particle, Eq. (1) for our case is a differential equation in two spatial variables. As has been done by others before [5,22–24], we express the PB equation in bispherical coordinates [25] since they are symmetry adapted to the geometric situation of the eccentric cell model. The BVP for the eccentric cell model then reads

$$\frac{(\cosh\eta-\cos\theta)^3}{b^2\sin\theta}\left(\partial_\eta\frac{\sin\theta}{\cosh\eta-\cos\theta}\partial_\eta+\partial_\theta\frac{\sin\theta}{\cosh\eta-\cos\theta}\partial_\theta\right)\Phi(\eta,\theta)=4\pi\lambda_B\left[(n_s+n_c)\frac{e^{\Phi(\eta,\theta)}}{\langle e^{\Phi}\rangle}-n_s\frac{e^{-\Phi(\eta,\theta)}}{\langle e^{-\Phi}\rangle}\right],$$

$$\partial_\theta\Phi(\eta,\theta)\big|_{\theta=0}=0,$$

$$\partial_\theta\Phi(\eta,\theta)\big|_{\theta=\pi}=0,$$

$$\partial_\eta\Phi(\eta,\theta)\big|_{\eta=\eta_0}=-\frac{Z\lambda_B}{a^2}\frac{b}{\cosh\eta-\cos\theta}, \tag{7}$$

$$\partial_\eta\Phi(\eta,\theta)\big|_{\eta=\eta_1}=4\pi\sigma_{out}\lambda_B\frac{b}{\cosh\eta-\cos\theta},$$

where

$$b=a\sinh\eta_0. \tag{8}$$

Like spherical coordinates, bispherical coordinates have two angle coordinates θ and ψ and a third coordinate η that has the character of a radius; i.e., the coordinate surfaces of the η coordinate are again simple spheres, with their centers being a function of η. Both the surface of the spherical WS cell and the surface of the macroion correspond to one η coordinate surface. In the (η,θ) system, this means that the region external to the macroion is a *rectangular* domain which is confined by η_0 (surface of macroion) and η_1 (surface at R') and $\theta=0$ and $\theta=\pi$.

The first two boundary conditions in Eq. (7) follow from symmetry considerations, while the last two ones are the constant charge boundary conditions on the colloid (charge Z) and the cell (charge density σ_{out}).

IV. DENSITY PROFILES

We discretize Eq. (7) and solve it numerically [26]. The nonlinearity is handled by a Newton-Raphson iteration scheme. Our numerical scheme resembles that of Carnie *et al.* [5] where a detailed discussion of the numerical procedure to solve PB in bispherical coordinates can be found.

Concerning the choice of our coordinate system two further comments are perhaps in order. First, a uniform grid in the domain of the bispherical coordinates leads to a particularly high density of node points in the region where we expect the variations of the ionic profile to be most pronounced, namely, in the region where the colloidal particle approaches the outer surface. Second, due to the steep slopes of the profiles near the colloid surface, care must be exercised to have an sufficiently fine grid in this region. A coordinate that is not adapted to the spherical symmetry of the colloid, as, for instance, the usual Cartesian coordinate system, would invariably lead to material grid errors near the curved surface of the colloidal sphere.

A simple uniform grid in the (η,θ) plane proves to be sufficient for relatively small macroionic charges ($Z<500$). For higher charges, we use a nonuniform grid in the (η,θ) plane which, after each iteration cycle, is readjusted to the gradient of the density profile so as to ensure that the number of node points corresponds to the steepness of the profile. The total number of node points is varied from 1000 up to 4000 until a sufficient accuracy is achieved.

Figure 2(a) displays a typical counterion density distribution calculated from Eq. (7). The volume of the WS cell corresponds to a volume fraction of the colloidal suspension of $\phi=0.05$. λ_B is 7.2 Å. The macroion (radius $a=500$ Å) is displaced a distance of $X=0.69R$; its charge is $Z=600$, and the salt concentration is zero ($S=0$). Figure 2(b) shows a cut through the distribution of Fig. 2(a) along the x direction at $y=0$. Both figures reveal that the density distribution has the expected shape, with a thick layer of (''condensed'') counterions in the vicinity of the macroion surface and an asymmetric valley between the colloidal surface and the outer, confining surface. Note that the density at the left-hand side (LHS) of the colloid in Fig. 2(b) is significantly larger than on the RHS. The charge asymmetry has a twofold effect: first, with the center of negative charge being different from the center of positive charge, the whole cell has an effective dipole moment and there will be electric field lines in θ direction at the cell boundary. And, second, the osmotic pressure will also have an (η,θ) dependence. Both will contribute to the electric stress tensor, and will lead to a net force directed towards the center of the WS cell.

A convenient way to check the implementation of the numerical scheme is to consider the case $X=0$ and compare the resultant profile with the solution to the BVP of Eq. (6). We have successfully performed these checks.

V. CAVITY FORCES AND FORCE CONSTANTS

The net force acting on the colloid inside the cell is the accumulated force of all 12 neighbors that make up the cage, or cavity, at R'. To distinguish it in the following from the pair forces, let us call this net cumulative force the ''cavity force.'' It is the derivative of $\mathcal{F}$ with respect to X, Eq. (3),

$$F_c(X)=-\frac{d}{dX}\mathcal{F}(X), \tag{9}$$

where $\mathcal{F}$ is calculated from the density profile using Eq. (2). Alternatively, we can calculate this force by means of the stress tensor,

$$\vec{\vec{T}}=\left(\Pi+\frac{\epsilon}{8\pi}E^2\right)\vec{\vec{I}}-\frac{\epsilon}{4\pi}\vec{E}\vec{E}, \tag{10}$$

which we have to integrate over a surface S that encloses the central colloid,

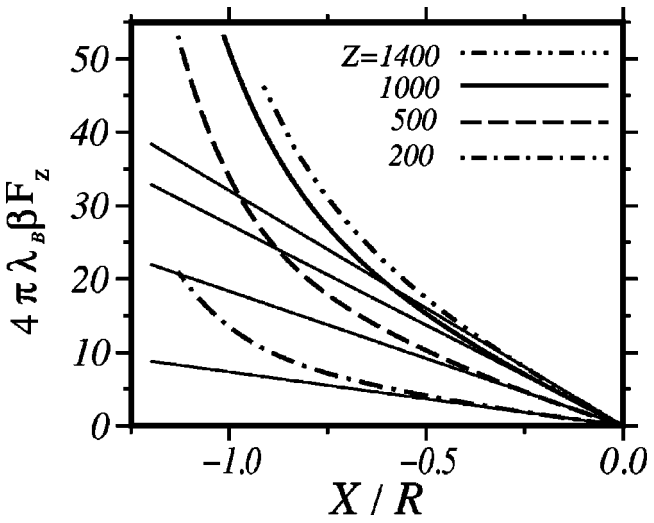

FIG. 3. Cavity forces (dimensionless) calculated from ion density distributions by integration of the stress tensor, as a function of the displacement X of the central colloidal particle. Force curves for several charges of the macroion (no salt) are shown, together with the linear forces (thin solid lines) calculated in the harmonic approximation, Eq. (14) ($a=500$ Å, volume fraction $\phi=0.05$).

$$\vec{F}_c=\int_S \vec{\vec{T}}\cdot\vec{n}\,dS. \tag{11}$$

It is $\vec{E}=E_\theta\vec{e}_\theta+E_\eta\vec{e}_\eta=-\vec{\nabla}\Psi$ the electric field and Π the local osmotic pressure which is equal to $kT(\rho_++\rho_-)$. The vector $\vec{n}$ is a unit vector directed normal to the surface S (inward direction). For convenience, we integrate over an η coordinate surface ($\eta=\eta_2$, with $\eta_1<\eta_2<\eta_0$). Clearly, the force is directed along the x axis and reads, when written in the usual dimensionless form,

$$f=4\pi\lambda_B\beta F_c=\pi e^2\beta^2\int_0^\pi\left[\left(\frac{8\pi}{\epsilon\beta}\rho+E_\theta^2-E_\eta^2\right)\times(1-\cos\theta\cosh\eta_2)+2E_\theta E_\eta\sinh\eta_2\sin\theta\right]\times\frac{\sin\theta}{(\cosh\eta_2-\cos\theta)^3}\,d\theta, \tag{12}$$

where all three functions E_θ, E_η, and ρ depend on (η_2,θ). As for the choice of η_2, the result should, in theory, be independent of η_2. In practice, this is hard to achieve because of numerical errors. They show up very clearly when f is plotted as a function of η_2 which is a good method to monitor the accuracy of the calculation.

Figure 3 shows the cavity forces as a function of the displacement X obtained from the density profiles by integration of the stress tensor. We consider colloidal charges ranging from $Z=200$ to $Z=1400$ in a suspension of volume fraction $\phi=0.05$ (no salt). The radius of the colloid is $a=500$ Å. We carefully checked that our results are free from grid errors. The numerical results have been double checked by calculating the cavity force via both routes, Eq. (9) and Eq. (12).

It is instructive to compare these curves with the forces calculated in the harmonic approximation when X is small and F_c becomes proportional to the displacement, $F_c=kX$. The force constant k in turn is related to the static rigidity G_s through $G_s=k/V_{WS}$ (see Ref. [18]; for the high frequency shear modulus see Ref. [19]). Interestingly, the force constants can already be found from the solutions to the usual spherical PB equation, Eq. (6), as has been pointed out in Ref. [27]. With Φ_0 being the solution to Eq. (6), integrated up to R' now, and r and θ being the usual spherical coordinates measured from the center of the cell, the electrostatic potential in linear approximation can be written in the form

$$\Phi(r,\theta)=\Phi_0(r)+\Phi_1(r)\cos\theta, \tag{13}$$

where the function Φ_1 is proportional to X and does not depend on θ. Inserting this into the PB equation for the eccentric geometry and expanding the inhomogeneity of the differential equation up to first order leads to a linear differential equation for $\Phi_1(r)$ whose integration provides us with an integral representation of Φ_1 in terms of the known potential Φ_0 (see Ref. [27]). Evaluating then the stress tensor with the potential of Eq. (13) and performing the surface integral, we find the following expression for the force in linear approximation:

$$4\pi\lambda_B\beta F_c(X)=-\frac{4\pi}{3}X\left\{\int_a^{R'}\frac{2+4\pi\lambda_B s^2\rho(s)}{s^4\Phi_0'^2(s)}ds\right\}^{-1}, \tag{14}$$

where $\rho(r)$ is the counterionic concentration profile in r proportional to $e^{\Phi_0(r)}$. Note that the expression is given for the salt-free situation only. Equation (14) now enables us to calculate forces for small X from a simple BVP, namely, the ordinary spherical BVP of Eq. (6). This therefore represents a way to determine forces that is completely independent of our way via the BVP in Eq. (7) and expression (12). As is evident from Fig. 3, the forces obtained from Eq. (14) give the correct result for small displacements. This may be seen not only as a verification of our results, but also as a confirmation of Eq. (14) which indeed provides a simple way to calculate force constants in colloidal crystals. Figure 3 also reveals that the X range where this perturbation approach is valid becomes smaller with increasing charge.

VI. PAIR FORCES

We now want to use the cavity forces presented in the last section to estimate the effective colloid-colloid interaction. Integration of Eq. (9) provides us with the function $\mathcal{F}(X)$ which, for a convenient notation, we abbreviate in the following by $U(X)$ [the constant $\mathcal{F}_0$ of Eq. (4) cannot be found by this integration and is set to zero in the following.] How can we come from $U(X)$, the total interaction energy between the central colloid and its 12 neighbors, to the effective pair potentials $u(r)$ between two dressed colloids?

Since we have replaced the 12 neighboring colloids by a spherical shell at $R'=2R-a$ with a continuous charge smeared out over the shell surface, we must assume that $U(X)$ is related to $u(r)$ not via the usual discrete lattice sum, but through an integral of the following form:

$$U(X)=2\pi(2R)^2\int_0^{\pi}u(r'(X,\theta))P(\theta)\sin\theta\,d\theta, \quad (15)$$

where r' is the distance between the shifted colloid in the center and a point (ϕ,θ) (spherical coordinates) on a spherical surface at $2R$ (the centers of the neighboring colloids are on the surface of a sphere at $2R$). The integration over ϕ is already performed. $P(\theta)$ is the probability of finding a neighboring colloid at the outer surface and is simply equal to $12/[4\pi(2R)^2]$. Realizing that $r'^2=(2R\cos\theta+X)^2+(2R\sin\theta)^2$, this integral can be further simplified and, after differentiation with respect to X, then provides us with the relation

$$X\partial_X U(X)+U(X)=\frac{12}{4R}[u(2R+X)(2R+X)+u(2R-X)\times(2R-X)]. \quad (16)$$

From this equation, we directly infer that there is no unique way to extract from U the functional form of u. We therefore depend on an *a priori* assumption of this form, and this is, of course, the assumption that for small X, u should be Yukawa like,

$$\beta u(r)=C\frac{e^{-\kappa r}}{r}, \quad (17)$$

with the two yet undetermined quantities κ and C. Since we consider the limit $X\to 0$, we expand either side of Eq. (16) to fourth order and find

$$\beta U_0+\frac{3}{2}k_2X^2+\frac{5}{4}k_4X^4=12\beta u(2R)\left(1+\frac{\kappa^2X^2}{2}+\frac{\kappa^4X^4}{24}\right), \quad (18)$$

where

$$\beta U(X)=\beta U_0+k_2X^2/2+k_4X^4/4+\cdots. \quad (19)$$

Comparison of the coefficients in front of X^2 and X^4 then leads to

$$\kappa^2=10\frac{k_4}{k_2},\qquad C=\frac{3}{10}\frac{k_2^2}{k_4}\frac{2Re^{2\kappa R}}{12}, \quad (20)$$

plus the obvious result $\beta U_0=12u(2R)$. Equation (20) thus gives a relation between the screening parameter κ and the prefactor C, on the one hand, and the force constants of $U(X)$ and their first anharmonic correction on the other.

With the parameters κ and C thus determined, we have arrived at effective pair potentials that are consistent with the cavity forces calculated in our eccentric cell model. To demonstrate that, we have plotted in Fig. 4 the total effective potential energy, obtained from integrating the force curves of Fig. 3, and compared it with the approximated energy function,

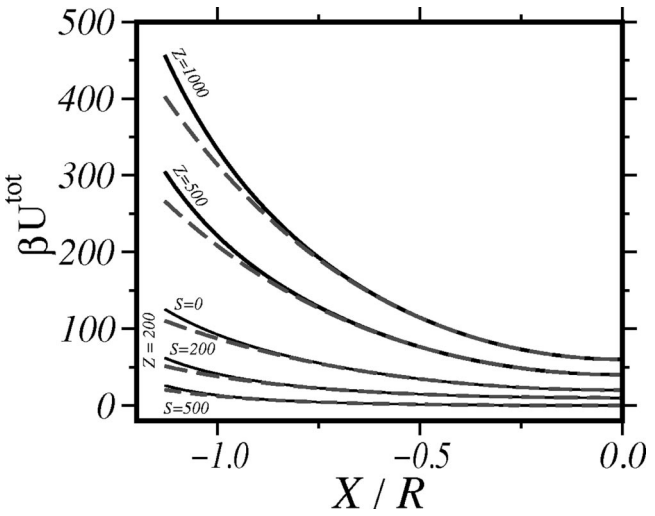

FIG. 4. Total potential energy (in units of $kT=1/\beta$) of the system (thick solid lines) as a function of X as obtained from integrating the cavity forces in Fig. 3. The dotted lines give an approximated energy derived from a superposition of Yukawa-like pair potentials; see Eq. (21). The colloidal charge is $Z=200$, $Z=500$, and $Z=1000$. For $Z=200$, two further calculations including salt ($S=200$ and $S=500$) have been performed.

$$\beta U^{tot}(X)=12C\frac{e^{-\kappa 2R}}{\kappa 2R}\frac{\sinh\kappa X}{X}, \quad (21)$$

which is obtained when the pair potential of Eq. (17) is inserted into Eq. (15). Figure 4 confirms that the pair potentials of Eq. (17), when superposed in the form of Eq. (15), can account for the calculated total energies over fairly a large range of displacements. This, of course, can also be seen as a statement about the validity of the expansion in Eq. (19).

In Fig. 5, the potential parameters C and κ are plotted as a function of the structural colloidal charge Z for two salinities $S=0$ and $S=200$ ($n_s=3\times10^{-5}M$). The Yukawa potential curves $\beta u(r)$ of Eq. (17) are plotted in Fig. 6. The corresponding DLVO results are given for comparison. The effective or renormalized values for the charge Z_{eff} and screening constant $\kappa=[4\pi\lambda_B(Z_{eff}+2S_{eff})/V_{WS}]^{1/2}$ in the DLVO potential, Eq. (5), have been calculated from the centric PB profiles according the prescriptions of Alexander *et al.* [9]

In Fig. 5, the standard DLVO or centric PB curves present the well-known saturation behavior of the renormalized charges, which, in turn, can be traced to the nonlinear phenomenon of counterion condensation. This phenomenon is, of course, also present in our calculation, as we have noticed already in the density plots of Fig. 2. It comes to light another time in Fig. 3, where we observe that the force constants also appear to saturate with increasing Z. [With Eq. (14), this comes as no surprise, since the force constants can be obtained from Φ_0, the solution to the spherical PB equation, and thus must also show saturation.] What is surprising, however, is that not only the force constant k_2, but also the anharmonic constant k_4 has this behavior. Both quantities k_2 and k_4 have the same dependence on Z. Since κ is related to the ratio of k_4/k_2, Eq. (20), it must therefore become a constant. From Fig. 5 we learn that it is a constant over the entire Z range. Contrary to the screening parameters, comparison of

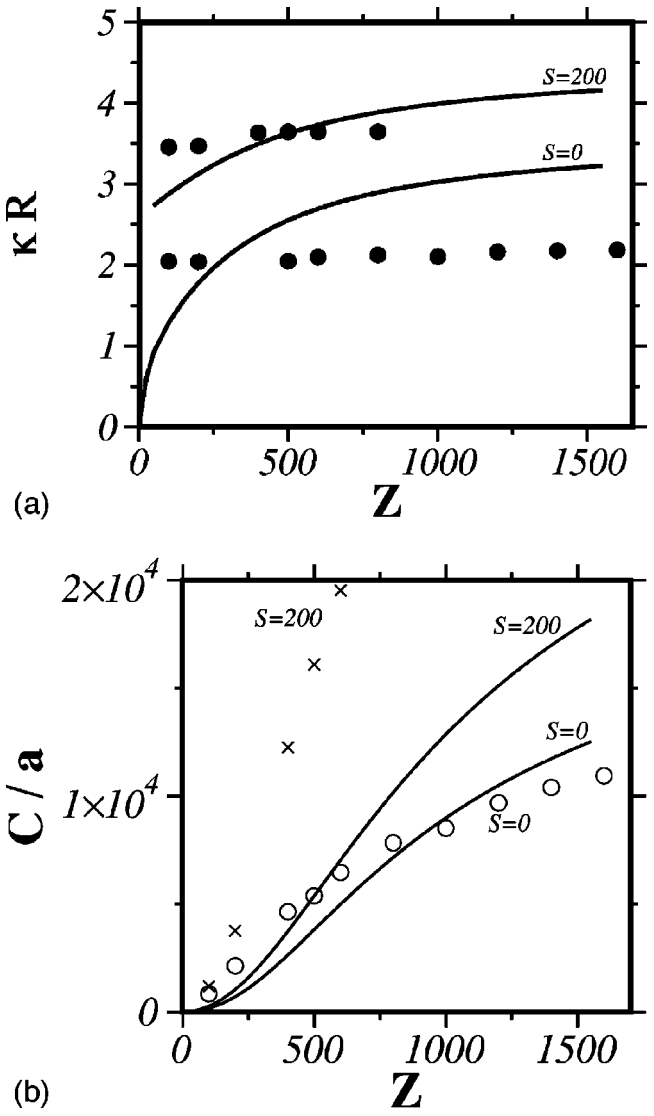

FIG. 5. Dependence of the screening parameter κ (a) and the prefactor C (b) of the Yukawa pair potential on the colloidal charge for two different salt concentrations. The screening parameter derived in the standard PB cell model (thick lines) depends on the effective charge [9] and shows the typical saturation behavior due to counterion condensation. In the eccentric cell model, the interaction between the double layers of the colloid and the outer surface leads to a screening that is independent of Z (solid circles).

the prefactors reveals only quantitative differences between both models: qualitatively the curves are similar, in particular for $S=0$.

In Fig. 6, it can be seen that for all Z, the difference between our results and the DLVO pair potentials is considerable, mainly because of the different Z dependence of κ. At this point, it is important to note the difference between our approach and that of Alexander et al. In the centric geometry, there is no force calculation. Using the picture of Alexander *et al.* to calculate the effective charges and putting it in the DLVO potential is certainly an attractive, illustrative but nevertheless phenomenological approach. There is no proof that the pair force is correctly given by this procedure. In our eccentric geometry, we calculate $F(X)$, a real force, which, of course, is still based on a number of crude approximations. However, it is a force and can subsequently be decomposed into pair forces. Furthermore, we not only take account of the effect of counterion condensation, but allow for the overlap between the double layer of the central colloid and the superposed layers of the cage colloids. We thus go beyond the centric model, and, accordingly, our pair potentials should be nearer to the experimental data than those calculated in the centric model.

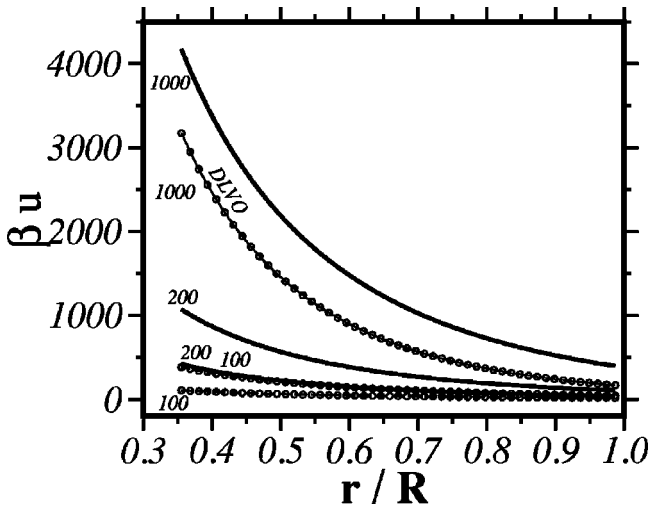

FIG. 6. Ion-averaged colloid-colloid pair potentials derived in the eccentric cell geometry (solid line) and using the effective-charge concept [9] (line with symbols) in the DLVO potential, for three different values of the colloidal charge.

To sum up, the result of Fig. 5 suggest that in the case of highly concentrated suspensions, where it is not sufficient to consider the interaction of two colloids well separated from the rest of the suspension, the multibody interaction between different colloids can result in a qualitatively different screening behavior, with a screening parameter that is to leading order independent of Z. The total magnitude of the potential is found to be somewhat different for highly charged spheres than predicted with the phenomenological renormalization scheme of Alexander *et al.*

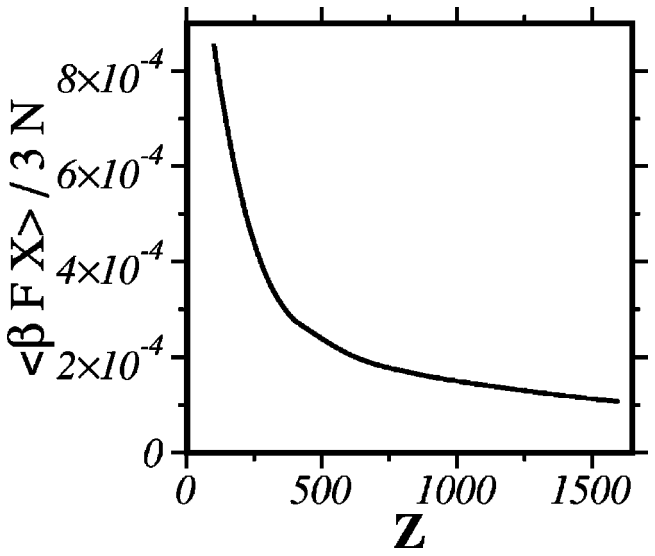

FIG. 7. The virial contribution of the colloidal particle to the osmotic pressure of a charge-stabilized colloidal suspension.

VII. OSMOTIC PRESSURE

Until now, we have focused on the forces acting on the particles. From our profiles, we can also extract information on the osmotic pressure. Treating polyions (mean density n_p) and microions (density n_{ion}) on equal footing (as one does in the primitive model), one would obtain the pressure from the virial equation

$$\beta p = n_p + n_{ion} + \frac{\beta}{3V}\left\langle \sum_p \vec{R}_p \vec{F}_p \right\rangle + \frac{\beta}{3V}\left\langle \sum_i \vec{r}_i \vec{F}_i \right\rangle, \tag{22}$$

where $\vec{R}_p$, $\vec{r}_i$ and $\vec{F}_p$, $\vec{F}_i$ are the positions of and the forces on the polyions and the microions, respectively. In the centric PB cell model the polyions are frozen in a perfect fcc configuration; thus the forces on the colloidal particles are zero. The rest of Eq. (22) then reduces to just the microion density at the cell edge,

$$\beta p = \rho_{ion}(R). \tag{23}$$

In the eccentric cell model considered here, the fcc lattice is not perfect and the forces on the colloidal spheres do not vanish. We therefore have the possibility to estimate the error made by neglecting the contribution of the colloids to the osmotic pressure [third term in Eq. (22)]. With the forces $F_c(X)$ of Eq. (11), we can calculate

$$\frac{\beta}{3N}\langle \vec{X}\cdot\vec{F}_c(X)\rangle = \frac{\beta}{3N}\frac{\int XF_c(X)e^{-\beta U(X)}X^2dX}{\int e^{-\beta U(X)}X^2dX}, \tag{24}$$

where N is the total number of microions in our cell. This can be compared with the contribution of the microions to the osmotic pressure coefficient, $\rho(R)/(N/V_{WS})$. Figure 7 shows that $(\beta/3N)\langle \vec{X}\cdot\vec{F}_c(X)\rangle$ drops rapidly from 10^{-3} for $Z=100$ to 10^{-4} for $Z=1000$. This compares to values for $\rho_{ion}(R)/(N/V_{WS})$, Eq. (23), dropping in the same range from 0.9 to 0.3, so that the contribution of the colloids to the osmotic pressure ranges between 10^{-3} and 10^{-4}. This, indeed, is a negligible quantity.

VIII. CONCLUSION

We have calculated the force that is experienced by a charged colloid inside a spherical charged cavity filled with an electrolyte. This force results from the overlap of the convex double layer around the colloidal particle and the concave double layer near the confining sphere. This concave double layer—and that is the key idea of this paper—is our approximation for the form of a double layer that results from the superposition of double layers of all 12 neighbors. The total force on the center colloid has subsequently been decomposed into effective pair forces, which thus gives an approximation of the effective ion-averaged potential in the high concentration limit, where the pairwise interaction between any two colloids is strongly influenced by the presence of all other polyions in the suspension. Comparing the charge dependence of the screening parameter in both the centric and the concentric PB cell models, we have found that the screening behavior in this high concentration limit shows a qualitatively different screening behavior. We have, furthermore, calculated the force constants and the anharmonic correction terms, and considered the contribution of the colloidal particles to the osmotic pressure of the suspension.

[1] L. Belloni, Colloids Surf. A **140**, 227 (1998).
[2] H. Löwen and J.P. Hansen, Annu. Rev. Phys. Chem. (to be published).
[3] K.S. Schmitz, *Macroions in Solution and Colloidal Suspension* (VCH, New York, 1993).
[4] G. Nägele, Phys. Rep. **272**, 215 (1996).
[5] S.L. Carnie, D.Y.C. Chan, and J. Stankovich, J. Colloid Interface Sci. **165**, 116 (1994).
[6] J.L. Barrat and J.F. Joanny, Adv. Chem. Phys. **94**, (1996).
[7] E.J.W. Verwey and J.T.G. Overbeek, *Theory of the Stability of Lyphobic Colloids* (Elsevier, Amsterdam, 1948).
[8] G.M. Bell, S. Levine, and L.N. McCartney, J. Colloid Interface Sci. **33**, 335 (1970).
[9] S. Alexander, P.M. Chaikin, P. Grant, G.J. Morales, P. Pincus, and D. Hone, J. Chem. Phys. **80**, 5776 (1984).
[10] L. Belloni, J. Chem. Phys. **85**, 519 (1986).
[11] M.O. Robbins, K. Kremer, and G.S. Grest, J. Chem. Phys. **88**, 3286 (1988).
[12] R. Krause, B. D'Aguanno, J.M. Mendez-Alcaraz, G. Nägele, and R. Klein, J. Phys. Chem. **3**, 4459 (1991).
[13] M.J. Stevens, M.L. Falk, and M.O. Robbins, J. Chem. Phys. **104**, 5209 (1996).
[14] F. Blitzer, T. Palberg, H. Löwen, R. Simon, and P. Leiderer, Phys. Rev. E **50**, 2821 (1994).
[15] M. Evers, N. Garbow, D. Hessinger, and T. Palberg, Phys. Rev. E **57**, 6774 (1998).
[16] M. Fushiki, J. Chem. Phys. **97**, 6700 (1992).
[17] H. Löwen, J.P. Hansen, and P.A. Madden, J. Chem. Phys. **98**, 3275 (1993).
[18] T. Ohtsuki, S. Mitaku, and K. Okano, Jpn. J. Appl. Phys. **17**, 627 (1977).
[19] A. Goodwin, J. Chem. Phys. **85**, 559 (1986).
[20] B. Beresford-Smith, D.Y. Chan, and D.J. Mitchell, J. Colloid Interface Sci. **105**, 216 (1984).
[21] R. van Roij, M. Dijkstra, and J.P. Hansen, Phys. Rev. E **59**, 2010 (1999).
[22] L.N. McCartney and S.J. Levine, J. Colloid Interface Sci. **30**, 345 (1969).
[23] J.E. Ledbetter, T.L. Croxton, and D.A. McQuarrie, Can. J. Chem. **59**, 1860 (1981).
[24] H.H. von Grünberg, J. Phys.: Condens. Matter (to be published).
[25] P. Moon and D.E. Spencer, *Field Theory Handbook*, 2nd ed. (Springer, Berlin, 1971).
[26] E.N. Houstis, W.F. Mitchell, and J.R. Rice, ACM Trans. Math. Softw. **11**, 379 (1985).
[27] V. Reus, L. Belloni, T. Zemb, N. Lutterbach, and H. Versmold, J. Phys. II **7**, 603 (1997).